

## Review

# What nano-physical properties can be determined by analysis of elastic peak accompanied by its inelastic background tail in XPS and AES spectra?

Shaaker Hajati and Sven Tougaard

*Department of Physics and Chemistry, University of Southern Denmark,  
DK- 5230 Odense M, Denmark*

(Received: May 8, 2006 ; Accepted: July 1, 2006)

We review examples of analysis of XPS and AES spectra based on analysis of the peak shape to show the ability of this method to quantify several physical properties of nano-particles and nano-structured thin films. This includes determination of IMFP, amount of substance, thickness of thin films and identification of growth mechanism of adsorbates.

Comparison with other techniques; ARXPS, RBS, AFM, XTEM and QCM as well as advantages and disadvantages of each technique are discussed.

## 1. Introduction

Recently, the technological importance of surface nano-structures has increased considerably, in many fields of application. Electron spectroscopy provides promising possibilities for quantitative and non-destructive chemical characterization of surface nano-structures. Therefore, improvements in methods to store and share spectral data between laboratories [1] as well as to analyze the data are required. Due to understanding of electron scattering processes in the surface region of solids, the accuracy of the non-destructive in-depth analysis of thin-layer structures has improved and novel, accurate quantitative methods have appeared. One of the existing methods for non-destructive determination of surface composition-depth profiles are based on the analysis of the part of the spectrum that is attributable to the contribution of electron scattered inelastically in the solid (inelastic background analysis [2-8]). Analysis of shape and intensity of inelastic background in XPS spectra was applied successfully previously for determining the nano-structure of metal films developed on semiconductors [9, 10], of metal/metal oxide films deposited on metals [11-14], of metal oxide films deposited on SiO<sub>2</sub> [15, 16] and of semiconductor layers formed on a semiconductor [17, 18]. The limits of validity of the technique used in these studies have been reviewed in Ref. [8]. The software package QUASES-Tougaard (Quantitative Analysis of Surfaces by Electron Spectroscopy) has been developed [19] as a general tool for this type of analysis. This technique probes depths up to ~ 10 inelastic mean free paths (IMFP).

Recently, Tougaard proposed a simplified algorithm,

which is also based on the dependency of background shape on the depth distribution [20]. This algorithm is less accurate than the former and gives less detailed information on the depth profile but it is suitable for automatic data processing. The validity of this simplified method was tested for XPS taken from different nano-structures and found to be in good agreement with results from other techniques [21]. These tests were performed for large XPS-spot size (~5 mm<sup>2</sup>).

The ability of the algorithm to study XPS with ~ 3 μm lateral resolution was successfully tested to give both an accurate image of the amount of substance (AOS) and several images of depth distributions of atoms (tomography) in the outermost few nano-meters of the sample [22].

Ref. [23] includes a good example to show the ability of QUASES-Tougaard software to, consistently, determine the same amount of Au atoms within the surface region of a series of solids where the depth distribution of a fixed number of Au atoms is varied. The samples were produced by first evaporating a few monolayers of gold onto the surface of a polycrystalline copper sample and then evaporating varying amount of copper on top. Systematic changes in peak intensity and in background were seen (see Fig. 1). By taking these changes into account in peak shape analysis of Au 4d peaks, the determined amount of gold of different depth distribution was found to be constant within a RMS deviation of 7%.

In comparison, traditional XPS-analysis based on peak intensity was applied and then a RMS deviation of 45% was found between the determined relative surface concentra-

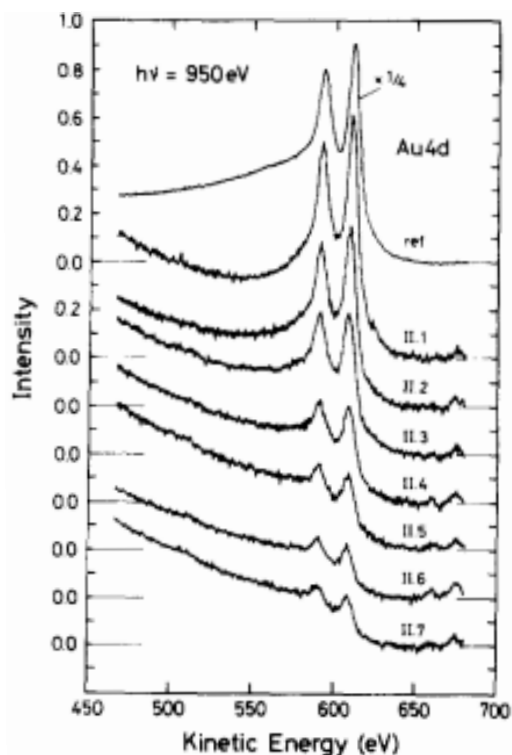


Fig.1 A thin Au layer on Cu with increasing amounts of evaporated Cu on top. Spectra corresponding to one set of measurements after being corrected for the energy dependence of the analyzer transmission function and after subtracting a straight line fitted on the high energy side of each peak. Notice that the Au 4d peak intensity decreases with increasing amount of evaporated copper. Also shown is the reference spectrum (ref.) from a pure polycrystalline gold sample. Excitation photon energy is 950 eV. Taken from Ref. [23].

tions for the set of samples which is in strong contradiction with the knowledge that the total amount of gold and thereby the average concentration within the surface region is identical for all samples.

If the surface structures and the in-depth distribution of atoms are known, the Tougaard method can be used to determine the electron IMFPs in such layers by analysis of a single spectrum [24-26].

Angle-resolved XPS (ARXPS)[27-32], also called the electron take-off angle (ETOA) method, is an alternative method for non-destructive quantification of the in-depth distribution of atoms. The method may be used to determine IMFPs if the in-depth distribution of atoms and/or surface structure is known from analysis with other techniques.

The peak shape analysis method requires only a single spectrum and therefore less diffraction effects for crystalline solids as well as less shadowing effect might be present, see Fig.2. On the other hand, the latter requires spectra to be recorded for a wide range of emission angles and therefore severe diffraction effects for crystalline solids as well as severe shadowing effect might be present. In other words, ARXPS requires amorphous and flat surfaces, see Fig.2.

In this review, some recent examples of analysis of XPS and AES spectra based on peak shape to show the ability of QUASES-Tougaard to quantify several physical properties of nano-structured thin films such as determination of IMFP, amount of substance (AOS), thickness of thin films and identification of growth mechanism of nano-structured overlayers. Comparison with other techniques; ARXPS, RBS, AFM, XTEM and QCM as well as advantages and disadvantages of the techniques are discussed.

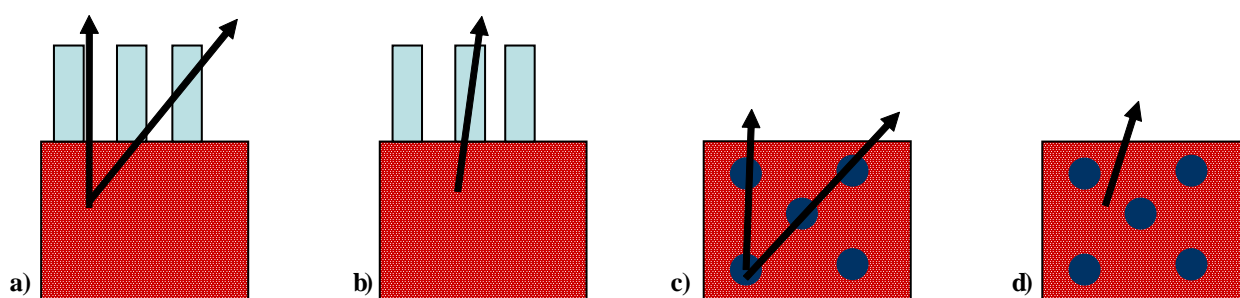


Fig.2 a) ARXPS-Analysis: Severe problems because of angle depending shadowing effect, very flat surfaces is required. b) Peak shape analysis: No problem with shadowing because only a single emission angle is used. c) Diffraction effect for crystalline solids can be a severe problem in ARXPS-analysis, therefore it requires amorphous surfaces. d) Diffraction effect for crystalline solids is less problematic in peak shape analysis because only a single emission angle is used.

## 2. Theory

A measured XPS spectrum  $J(E)$  was shown to be a function of the intrinsic distribution,  $F(E)$ , of primary emitted photoelectrons per angstrom, the differential inelastic scattering cross-section,  $K(T)$ , and the composition depth profile,  $f(x)$  [2]. For a correct quantitative analysis the intrinsic  $F(E)$  therefore has to be restored from  $J(E)$  by removal of extrinsic contributions under the assumption of the correct  $f(x)$  and  $K(T)$ . Alternatively  $f(x)$  can be evaluated from  $J(E)$ , if  $F(E)$  and  $K(T)$  are known. When the extrinsic contributions are removed correctly from  $J(E)$ ,  $F(E) \approx 0$  in a wide energy interval 50-150 eV on the low energy side of the peak. In situations where the effects of the chemical environment do not significantly affect the intrinsic shape of  $F(E)$ , the restoration process must give  $F(E)$  spectra similar in both intensity and shape in order to be correct.

The general solution for the extraction of  $F(E)$  from  $J(E)$  were described rigorously as follows and developed for different types of in-depth distributions [2-8,19]

$$F(E) = \frac{1}{P_1} \left\{ J(E) - \int dE' J(E') \int_{-\infty}^{+\infty} ds \exp(i2\pi s[E'-E]) \left[ 1 - \frac{P_1}{P(s)} \right] \right\} \quad (1)$$

where

$$P_1 = \int_0^{\infty} dx f(x) \exp\left(\frac{-x}{\lambda \cos \theta}\right) \quad (2)$$

and

$$P(S) = \int_0^{\infty} dx f(x) \exp\left(\frac{-x}{\lambda \cos \theta} \left[ 1 - \int_0^{\infty} dT \lambda K(T) \exp(-iT) \right] \right) \quad (3)$$

In the above equations,  $\theta$  is the angle of detection with respect to the surface normal and  $\lambda$  the inelastic mean free path (IMFP).

For  $K(T)$ , the following expression

$$\lambda K(T) = \frac{BT}{(C+T^2)^2} \quad (4)$$

with  $C=1643 \text{ eV}^2$  and  $B=3000 \text{ eV}^2$  is a valid approximation for many transition metals as well as for their alloys and oxides [33]. For solids such as Al, Si,  $\text{SiO}_2$ , and polymers that have a narrower cross section, it is a better approximation to use

$$\lambda K(T) = \frac{BT}{(C-T^2)^2 + DT^2} \quad (5)$$

where  $C$  and  $D$  are constants characteristic of the solid [33].

## 3. Determination of IMFP

### 3.1 The IMFP in the Langmuir-Blodgett (LB) film

QUASES-Tougaard was used to study a photopolymerized

cadmium 10,12-pentacosadiynoate monolayer Langmuir-Blodgett (LB) film, with monomer formula:  $(\text{CH}_3(\text{CH}_2)_{11}\text{C}\equiv\text{CC}\equiv\text{C}(\text{CH}_2)_8\text{COO})_2\text{Cd}$ , on top of a silicon wafer with a native oxide layer with twofold objective: to determine the ability of peak shape analysis to give consistent quantification when spectra from the same sample but taken at widely different emission angles were analyzed and thereby to conclude that the QUASES-Tougaard simply requires a spectrum taken at a single emission angle to give the same information as the ARXPS does using several emission angles from the same sample, and to determine IMFPs for electrons in the film at various energies. The latter is the focus of this section. Survey spectra were taken at several emission angles between  $5^\circ$  and  $78^\circ$  and then analyzed.

For each core level corresponding to the Si 2p, O 1s and Cd 3d photoelectron peaks with respective kinetic energies 1388 eV, 955 eV and 1082 eV, it was shown that the spectra taken at all angles of  $\leq 73^\circ$  give consistent quantification to within a standard deviation of 5-10%. This is approximately the same as the uncertainty in quantification made on the basis of a spectrum taken at a single angle. This demonstrates the robustness of peak shape analysis.

The surface structure and the thickness of the film were characterized by atomic force microscopy (AFM), as well as by ARXPS. From topmost surface layer to the bulk silicon (substrate), the respective layers were found to be hydrocarbon, Oxygen in COO, Cadmium ion, silicon dioxide and silicon bulk. The IMFP in this well-characterized LB film was also determined by the ARXPS method using relative atomic concentrations [32].

Using QUASES-Tougaard analysis, the IMFPs in the LB film were found to be  $29.2 \pm 1.7 \text{ \AA}$  at 955 eV and  $40.2 \pm 2.2 \text{ \AA}$  at 1388 eV. These values are close to those reported (using ARXPS) in ref. [32] of 34 and 45  $\text{\AA}$  for the same sample and the same energies.

### 3.2 The IMFP for high energy electrons (6000-7000 eV) in the Cu, Ni and Co thin films

Quantitative application of non-destructive electron spectroscopic methods in the high (5-10 keV) energy region are gaining an increasing importance recently, especially in the fields of determining thickness of metallic overlayers in several tens of nanometer region and of analyzing deeply buried interface layers. The availability of experimental IMFP values, which is important physical parameters for quantification, for electrons in this energy region, however, is limited.

This was studied in Refs. [25, 34] where, Cu, Ni, Co thin layers of 50-400  $\text{\AA}$  thickness on Si wafer substrate were prepared. High energy Co, Cu, Ni *KLL*, Co *KLM* Auger and Cu 2s, 2p and Si 1s photoelectron spectra were excited from the thin film samples using Cu characteristic ( $K\alpha_1$ ,  $K\alpha_2$ ) and bremsstrahlung X-rays.

Film thicknesses were obtained from independently experimental procedures using quartz crystal microbalance (QCM), and in the case of Cu and Ni using cross sectional transmission electron microscopy (XTEM) and scanning probe (atomic force) microscopy (SPM) [34]. Knowing the thickness, peak shape analysis was used to determine IMFP values of high energy photoelectrons (6000-7000 eV) within Cu, Ni and Co thin film samples, which gave consistent values for different overlayer thicknesses and transitions. The data from Powell and Jablonski [35], based on IMFPs calculated from experimental optical data as well as based on IMFPs measured by elastic peak electron spectroscopy (EPES), predict systematically higher IMFP values, however, the differences are only 10-20 % which is comparable to the expected error in both techniques.

#### 4. Growth mechanism

##### 4.1 Morphology of Ge islands on Si(001)

Study of growth mechanism of Ge on Si(001) are aimed at the possibility of creating coherent, self-assembled Ge islands of potential use in future optoelectronic device technology [36-38]. Therefore XPS inelastic peak shape analysis as well as atomic force microscopy (AFM) was applied to describe growth mechanism of Ge on Si as a function of temperature and Ge dosage [17, 18, 39]. In this section we present a short summary of these studies.

Substrate temperature was set at 200 °C, 550 °C and 700 °C. For each temperature, nominal Ge deposits of 5, 10 and 20 Å were produced, giving a total of nine differently prepared samples. For the structure investigation using inelastic peak shape analysis, Ge 2p was excited using Al K $\alpha$  and  $E_{\text{pass}} = 70$  eV, and Si KLL was excited using Mg bremsstrahl-

ung and  $E_{\text{pass}} = 250$  eV. Separate reference spectra were taken from pure Ge and Si.

The depth resolution of peak shape analysis is typically a few angstroms and the maximum probing depth is  $\sim 10$  IMFP in the more favourable cases [8, 14]. The lateral resolution of peak shape analysis is limited by the area probed by the electron energy analyzer (typically several mm) and structure information is averaged over this region. Note that peak shape analysis has recently been extended to provide images with  $\mu\text{m}$  lateral resolution [20-22]. Figure 3 shows the peak shape analysis of the Ge 2p and Si KLL spectra from a sample with 10 Å Ge deposited at 700 °C.

The island morphologies were found by both XPS and AFM which is summarized in Table 1. Within the uncertainty of the techniques there is good agreement between the results in most cases. The cases where a clear difference was found have been marked with \* and \*\*. For growth at 200 °C and 550 °C the island heights are consistent, but coverages are not. On the other hand, for 10 and 20 Å deposited at 700 °C island coverages are in agreement, whereas the height is not. The disagreements are attributed to the limitation of the respective techniques. These limitations are given mainly by the following two points:

\* The pronounced small-scale roughness of the Ge layer for low deposits [40] cannot be resolved by contact mode AFM because the tip size is larger than the lateral spacing between neighboring islands. But this roughness will correctly show up as islands in the peak shape analysis, regardless of the small scale. In addition, the information obtained by XPS analysis is the averaged information over a sample region of  $\sim 10 \times 10$  mm<sup>2</sup>. Thus height variation in the Ge film extending over large distances ( $\leq 10$ mm) will contrib

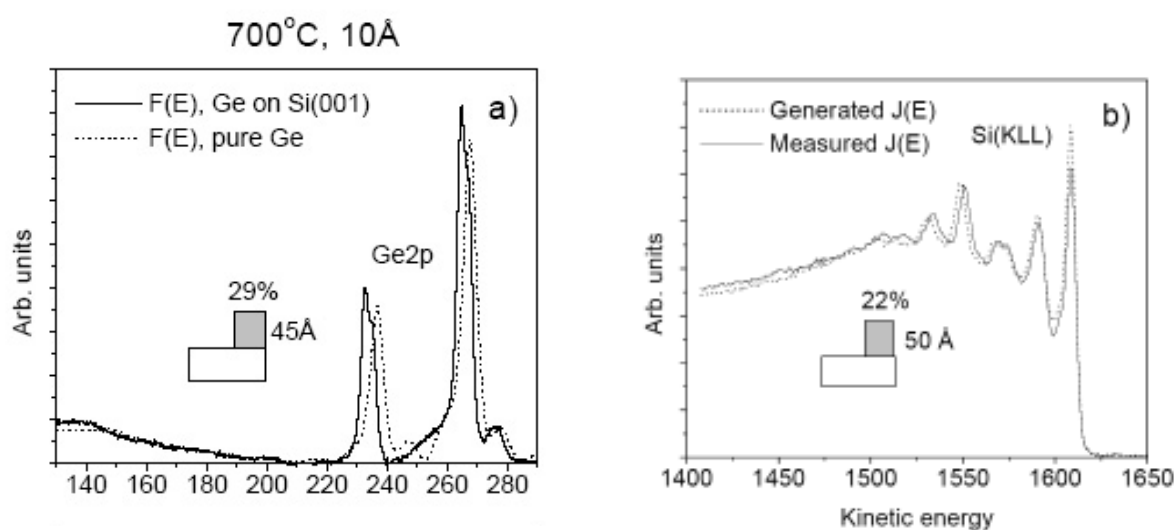


Fig.3 Inelastic peak shape analysis by XPS of the sample with nominally 10 Å of Ge deposited at 700 °C. Background subtraction (QUASES-Analyze) was used in the analysis of the Ge line (a) and spectrum synthesis (QUASES-Generate) was used for analyzing the Si KLL line (b). The island structures corresponding to the analysis are shown in each case. Owing to oxidation of the Ge film, the Ge 2p spectrum in (a) is shifted with respect to the spectrum from the clean Ge reference.

Table 1 Overview and comparison of film morphology determined by QUASES- Tougaard and AFM

Temperature	Ge deposit <sup>a</sup>	AFM		QUASES- Tougaard			
		Coverage (%)	Height (Å)	Coverage (%)		Height (Å)	
				Ge 2p	Si KLL	Ge 2p	Si KLL
700 °C	20 Å	32	200-400**	29	26	60**	90**
	10 Å	~20	50-200**	29	22	45**	50**
	5 Å	- <sup>b</sup>	- <sup>b</sup>	22	20	40	40
550 °C	20 Å	21	40-300	39	40	55	55
	10 Å	≤ 10*	40	36*	35*	35	40
	5 Å	≤ 10*	40	25*	30*	35	40
200 °C	20 Å	≤ 10*	55	58*	50*	45	50
	10 Å	- <sup>b</sup>	- <sup>b</sup>	39	40	37	35
	5 Å	- <sup>b</sup>	- <sup>b</sup>	29	35	30	30

<sup>a</sup>The Ge evaporation flux was constant during deposition and controlled using an Inficon Sentinel III flux controller. Calibration of the Ge flux was performed using separate RBS measurements.

<sup>b</sup>Samples where no structure could be resolved with AFM. Entries marked with \* and \*\* indicate a disagreement between the techniques that is explained further in the text.

ute to the XPS morphology in the same way as microscopic islands. However, such large-scale variations are not visible with AFM.

\*\* As mentioned before, the probing depth of the overlayer signal is 5-10 IMFP but for the substrate signal it is less. Altogether, this gives a maximum probing depth of 50-70 Å, in agreement with the results of Table 1. On the other hand, AFM can resolve much taller islands.

The disagreements found in Table 1, indicated with \* and \*\*, can in each case be attributed to one of the abovementioned points. Based on this, it was found that the detailed results of AFM are more accurate for samples with tall islands that can be resolved laterally (20 Å Ge at 550 °C and 700 °C). However, at lower deposits and lower temperatures the AFM resolution is insufficient and the XPS analysis gives more accurate information on the morphology.

The conclusion is that the morphologies determined with QUASES-Tougaard and AFM are consistent in most cases. The cases where disagreement is found can be explained by the complementarity of the techniques. Thus, the application of both techniques gives more complete information on the surface morphology.

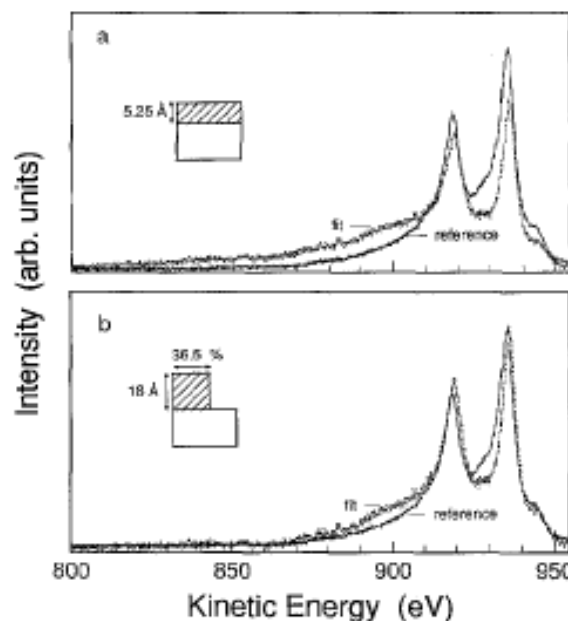


Fig. 4 Fits for Pt 4d using different structures. (a) Rectangular, 5.25 Å thick, layer on top of the substrate, (b) Single island is 18 Å high and covering 36.5% of the surface.

#### 4.2 Growth of thin Pt film on silicon at room temperature

The growth structure and interdiffusion of metallic layers into silicon is very difficult to determine by conventional surface analysis. The Pt 4d spectrum from a thin film of Pt evaporated on Si (111) at room temperature was taken and analyzed by using QUASES-Tougaard [41]. Analyzing the Pt 4d spectrum and requiring good agreement between the background corrected spectrum and the reference spectrum from the pure Pt sample for both the peak shape and the absolute intensity, the structure of the Pt film was determined. In Fig. 4 the spectrum for the deposited platinum are analyzed assuming two different growth models. Fig. 4a shows the best overall fit that could be obtained assuming a layer-by-layer growth model, namely a 5.25 Å thick rectangular layer on the surface. This is, however, too low in the peak region and too high in the background region. In Fig. 4b, the best fit assuming a single island model is shown. The island is 18 Å high and covering 36.5% of the surface. This is clearly a much better fit both at the peak and in the background. Within our uncertainties ( $\pm 5\%$ ) every other combination of structural parameters, e.g. using a lower coverage while simultaneously increasing the height gave worse fits.

In Fig. 5 it is shown how sensitive the fits are to a change of the structural parameters. In Fig. 5a the same height was used as in Fig. 4b, but the coverage was changed from 36.5% to 55%, while in Fig. 5b, the same coverage as in Fig. 4b was used but the height was changed from 18 Å to 12 Å. Both fits are clearly worse than the fit in Fig. 4b. This illustrates that the uncertainty on the determined structural parameters is quite low and in general the uncertainty is  $\sim 5\text{-}10\%$  [8]. The

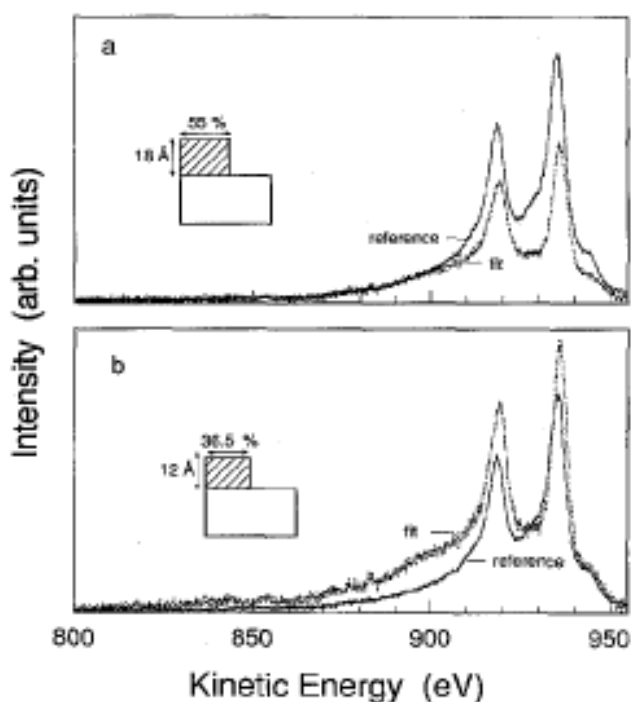


Fig. 5 Sensitivity of the fits to a change of the structural parameters.

conclusion is that Pt film growth is strong island formation which is fully consistent with the previously reported growth mechanism of Pt at room temperature [42, 43]

#### 5. Determination of Amount of substance (AOS) and/or the equivalent effective thickness and its consistency with other techniques:

##### 5.1 Analysis of $\sim 500\text{Å}$ thick Ni and Cu overlayer deposited on Si

As mentioned above, the inelastic background analysis probes depths up to  $\sim 10$  IMFP. For typical XPS peaks excited with Al  $K\alpha$  and Mg  $K\alpha$ , the IMFP is  $\sim 5\text{-}20$  Å and therefore the typical maximum probing depth is  $\sim 50\text{-}200$  Å. It is interesting to demonstrate the application of this method to larger overlayer thickness (metallic films having several tens of nanometer thickness) by analyzing the spectra of high energy transitions (excited by e.g. Cu X-ray) where  $\lambda$  is  $\sim 60$  Å, which is larger than for traditional XPS and Auger peaks, and therefore  $10\lambda$  is large,  $\sim 600$  Å. This was done in Ref. [34] where Ni and Cu KLL Auger spectra were photoexcited from Ni and Cu overlayers (deposited on Si substrates) of different thicknesses in the 100-600 Å range [34]. Spectra corresponding to 600 Å thick Ni and 400 Å thick Cu were taken as reference spectra. Fig. 6 is an example of analyzed spectrum from the thinnest Cu thin-film sample.

In QUASES-Tougaard analysis, IMFPs from Powell and Jablonski [35], was used to find the film thicknesses. These determined values were in good consistency with thicknesses determined by using a QCM and XTEM.

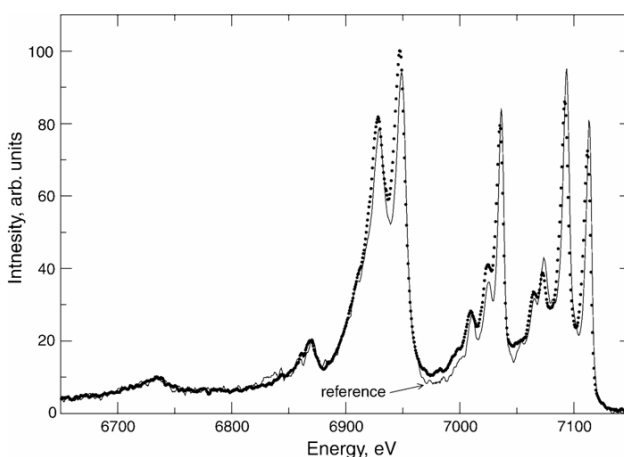


Fig. 6 Comparison of the source function  $F(E)$  obtained from the spectral shape analysis of the high-energy electron spectrum photoexcited from the thinnest Cu thin-film sample (assuming island growth) with the source function determined for the Cu reference sample. Taken from Ref. [34].

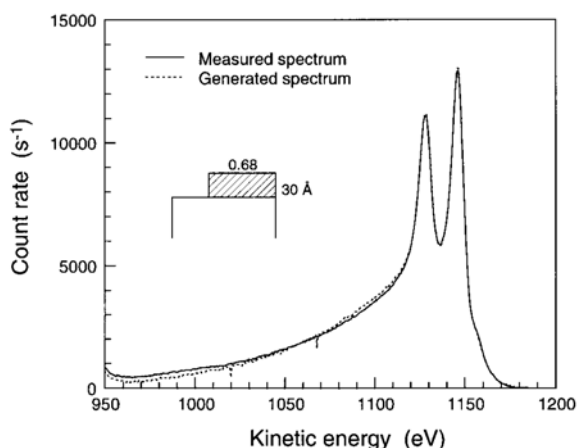


Fig. 7 Peak shape analysis of the Au 4d from an Au layer on Ni. The measured Au 4d spectrum (solid line) and the model spectrum (dotted line) which is calculated with QUASES-Generate based on an island model structure being 30 Å high and covering 68% of the sample surface.

Table 2 Quantitative parameters of the Au overlayer<sup>a</sup>

Sample no.	c (%)	h (Å)	$d_{\text{XPS}}$ (Å)	$\langle d_{\text{RBS}} \rangle$ (Å)
1	31	14	4.3	4.7
2	56	18	10.1	8.1
3	68	30	20.4	21.9
4	97	100	97	103.3
5	90	63	56.7	40

<sup>a</sup> The island coverage  $c$  and the island height  $h$  were determined by analysis of Au 4d peaks. The corresponding Au thickness  $d_{\text{XPS}}$  was determined from the XPS results, and the RBS Au thickness  $\langle d_{\text{RBS}} \rangle$  was determined as an average over the RBS measurements from different spots on one sample.

## 5.2 Determination of average thickness of Au layers deposited on Ni; A comparison with RBS

Rutherford backscattering spectrometry is a well-established technique with a high accuracy and low uncertainty [44] to quantify the amount of substance (AOS). Therefore, it is worth to show the degree of quantitative agreement between XPS peak shape analysis and RBS with respect to AOS of e.g. Au layers deposited on Ni [14]. Au amounts varying between 5 and 100 Å were evaporated to make different overlayers corresponding roughly to the in-depth

sensitivity range (0-10 IMFP) [8] of the peak shape analysis. For Au 4d excited by Al K $\alpha$  the value of  $\lambda$  is  $\sim 14$  Å and therefore the maximum probe depth is  $\sim 140$  Å. The appropriate amount of Au deposited onto the samples was controlled by measuring the Au 4d XPS peak during evaporation. The samples, hereafter labeled 1-5, had an equivalent Au thickness of 5, 10, 20, 100 and 50 Å, respectively. Study of the XPS Au 4d spectra acquired from these samples (see Fig. 7) give the results shown in Table 2 by simply considering the geometry of the islands additionally found for structure of the Au overlayers i.e.  $d_{\text{XPS}} = 0.01 \times c \times h$ . RBS measurements from several different regions of each sample were made for which result of analysis is also tabulated in Table 2.

For each sample, the agreement was characterized by the deviation between the results found by XPS ( $d_{\text{XPS}}$ ) and the mean value of the RBS results ( $\langle d_{\text{RBS}} \rangle$ ). For samples 1, 3 and 4 the deviation is 6-7%. For the remaining two samples the agreement is worse. The RBS results for different spots on samples 2 and 5 showed large variation in the thickness. This means that for these two samples the deposited Au layers are far from uniform whereas samples 1, 3 and 4 were quite uniform. Because the variation is much larger than the uncertainties of both XPS peak shape analysis and RBS, samples 2 and 5 are not suited for comparison. In other words, the disagreement between the XPS and RBS results found for samples 2 and 5 cannot be interpreted as a disagreement between the techniques.

In conclusion, the accuracy of the XPS peak shape analysis technique was found to be  $\sim 7\%$  for all depth  $\leq 7-8$  IMFP.

## References

- [1] K. Yoshihara and M. Yoshitake, *J. Vac. Sci. Technol. A*, **16**(3), 1388 (1998)
- [2] S. Tougaard, *Surf. Interface Anal.* **11**, 453 (1988)
- [3] S. Tougaard and H. S. Hansen, *Surf. Interface Anal.* **14**, 730 (1989)
- [4] S. Tougaard, *J. Vac. Sci. Technol. A* **8**, 2197 (1990)
- [5] S. Tougaard, *J. Electron Spectrosc.* **52**, 243 (1990)
- [6] S. Tougaard, *J. Vac. Sci. Technol. A* **14**, 1415 (1996)
- [7] S. Tougaard, *Appl. Surf. Sci.* **100/101**, 1 (1996)
- [8] S. Tougaard, *Surf. Interface Anal.* **26**, 249 (1998)
- [9] M. Schleberger, D. Fujita, C. Scharfschwerdt, S. Tougaard, *Surf. Sci.* **331**, 942 (1995)
- [10] M. Schleberger, D. Fujita, C. Scharfschwerdt, S. Tougaard, *J. Vac. Sci. Technol. B*, **13**, 949 (1995)
- [11] S. Tougaard, W. Hetterich, A. Nielsen, H. Hansen, *Vacuum*, **41**, 1583, (1989/1990)
- [12] H. Hansen, C. Jansson, S. Tougaard, *J. Vac. Sci. Technol. A* **10**, 2938 (1992)
- [13] S. Tougaard, H. Hansen, *Surf. Sci.* **236**, 271 (1990)
- [14] A.C. Simonsen, J.P. Pøhler, C. Jeynes, S. Tougaard, *Surf. Interface Anal.* **27**, 52 (1999)
- [15] F. Yubero, A. R. González-Elipé and S. Tougaard, *Surf.*

- Sci.* **457**, 24-36 (2000)
- [16] A.I. Martín-Concepción, F. Yubero, J.P. Espinós, A. R. González-Elipe and S. Tougaard, *J. Vac. Sci. Technol. A* **21**, 1393 (2003)
- [17] M. Schleberger, A.C. Simonsen, S. Tougaard, J.L. Hansen, A.N.Larsen, *J. Vac. Sci. Technol. A* **15**, 3032 (1997)
- [18] A.C. Simonsen, M. Schleberger, S. Tougaard, J.L. Hansen, A.N.Larsen, *Thin Solid Films* **338**, 165 (1999)
- [19] S. Tougaard, *QUASES-Tougaard: Software Package for Quantitative Analysis of Surface by Electron Spectroscopy*, Version 5.1 (2005). (see www.quases.com)
- [20] S. Tougaard, *J. Vac. Sci. Technol. A* **21**, 1081 (2003)
- [21] S. Tougaard, *J. Vac. Sci. Technol. A* **23(4)**, 741 (2005)
- [22] Shaaker Hajati, Sarah Coultas, Chris Blomfield and Sven Tougaard, *Surf. Sci.*, **600**, 3015 (2006)
- [23] F. Yubero, C. Jansson, D.R. Batchelor and S. Tougaard, *Surf. Sci.*, **331-333**, 753 (1995)
- [24] N. Suzuki, T. Kato, S. Tougaard, *Surf. Interface Anal.* **31**, 862, (2001)
- [25] L. Kövér, S. Tougaard, J. Tóth, D. Varga, O. Dragoun, A. Kovalik and M. Ryšavý, *J. Surf. Anal.* **9**, 281, (2002)
- [26] H.S. Hansen, S. Tougaard and H. Biebuyck, *J. Electron Spectrosc. Relat. Phenom.* **58**, 141 (1992)
- [27] P.J. Cumpson, *J. Electron Spectrosc. Relat. Phenom.* **73**, 25 (1995)
- [28] J.E. Fulghum, *Surf. Interface Anal.* **20**, 161 (1993)
- [29] L.B. Hazell, I.S. Brown, F. Freisinger, *Surf. Interface Anal.* **8**, 25, (1986)
- [30] N.G. Cave, R.A. Cayless, L.B. Hazell, A.J. Kinloch, *Langmuir*, **6**, 529, (1990)
- [31] M. Sastry, P. Ganguly, S. Badrinarayaman, A. B. Mandale, S.R. Sainkar, D. V. Paranjape, K. R. Patil and S. K. Chaudhary, *J. Appl. Phys.* **70**, 7073, (1991)
- [32] N. Suzuki, K. Iimura, S. Satoh, Y. Saito, T. Kato and A. Tanaka, *Surf. Interface Anal.* **25**, 650, (1997)
- [33] S. Tougaard, *Surf. Interface Anal.* **25**, 137 (1997)
- [34] L. Kövér, S. Tougaard, J. Tóth, L. Daróczi, I. Szabó, G. Langer and M. Menyhárd *Surf. Interface Anal.* **31**, 271, (2001)
- [35] C.J. Powell, A. Jablonski, *J. Phys. Chem. Ref. Data* **28**, 19 (1999)
- [36] E. Kasper, *Appl. Surf. Sci.* **102**, 189 (1996)
- [37] G. Abstreiter, P. Schittenhelm, C. Engel, E. Silveira, A. Zrenner, D. Meertens and W. Jäger, *Semicond. Sci. Technol.* **11**, 1521, (1996)
- [38] H. Sunamura, N. Usami, Y. Shiraki, S. Fukatsu, *Appl. Phys. Lett.* **66**, 3024, (1995)
- [39] A.C. Simonsen, S. Tougaard, J.L. Hansen, A.N.Larsen, *Surf. Interface Anal.* **31**, 328, (2001)
- [40] J. Knall, J.B. Pethica, *Surf. Sci.* **265**, 156, (1992)
- [41] M. Schleberger, D. Fujita, C. Scharfschwerdt and S. Tougaard, *Surf. Sci.*, **331-333**, 942 (1995)
- [42] P. Morgen, M. Szymonski, J. Onsgaard, B. Jørgensen and G. Rossi, *Surf. Sci.* **197**, 347 (1988)
- [43] R. Matz, R. Purtell, Y. Yokota, G. Rubloff and P. Ho, *J. Vac. Sci. Technol. A* **2**, 253 (1984)
- [44] C. Jeynes, Z. H. Jafri, R. P. Webb, A. C. Kimber, M.J. Ashwin, *Surf. Interface Anal.* **25**, 254 (1997)